Vector Reticle, Control Action Display in Manual Control of Space Vehicle Attitude

ROBERT H. CANNON JR.*
Stanford University, Stanford, Calif.

AND

WALTER G. EPPLER JR.†
Lockheed Missiles and Space Company, Palo Alto, Calif.

Two concepts, the vector reticle and control action display, are submitted as effective means for making manual three-axis attitude control quicker and more efficient while reducing substantially the concentration required of the pilot. A system design is submitted in which the two concepts are combined in a control action reticle and in which the pilot has direct control of the jet valves. (The entire system may be mechanical.) The system is controlled to a visual reference or to an instrument attitude reference. Malfunction of the system cannot interfere with normal manual control. The vector recticle presents all auxiliary information in a single three-part geometric vector superimposed on the window (rather than on three separate dials, for example), thus reducing the number of quantities to be monitored from three to one. Control action display gives the pilot instantaneous and exclusive control of the reticle, thus removing the need for two mental integrations and greatly reducing the concentration required for tracking. Results are presented of three-axis (fixed-base) simulation studies of the proposed system and of other systems for comparison.

Nomenclature

b = damping constant of dashpot between hand controller and moment control valve (Fig. 8), ft-lb-sec/rad
D_{1i} = rate display gain for system employing quickening, sec
D_{2i} = acceleration display gain for system employing quickening, sec^2
$G_d(s)$ = the part of the open loop transfer function which can be specified by the designer [Eq. (23)], sec^2
I_i = moment of inertia about a principal axis, slug-ft^2
K_{ci} = hand controller gain
K_d = open loop gain specified by the designer [Eq. (22)], sec^2
$KG(s)$ = open loop transfer function of single-axis attitude control system
K_i = proportionality constant for rate command mode, sec^{-1}
K_{ni} = ratio of lead time constant to lag time constant in compensation network
K_{mi} = gain for the proportional thrust control system relating control moment to valve opening, ft-lb/rad
K_{ri} = autopilot gain in rate command mode, ft-lb-sec/rad
k_1 = spring constant of spring between hand controller and moment control valve (Fig. 8), ft-lb/rad
k_2 = spring constant of spring across moment control valve (Fig. 8), ft-lb/rad
M_i = control moment exerted by reaction control system about a principal axis, ft-lb
M_{0i} = fixed value of control moment exerted by the on-off reaction control system about a principal axis, ft-lb
r = distance between window and pilot's eyes (Fig. 3), ft
T = minimum time required to correct initial offset angle in system employing on-off moment control, sec
α = angle between roll axis and projection of line of sight onto the vehicle yaw plane (Fig. 3a), rad
δ_i = hand controller deflection angles (Fig. 5), rad
ϵ = angle between line of sight and its projection onto the vehicle yaw plane (Fig. 3a), rad
ζ = damping ratio of second-order system
θ_i = reticle position referred to body axes (Fig. 4a), rad
ρ = angular rotation about the line of sight measured with respect to a plane parallel to the vehicle pitch plane (Fig. 3a), rad
τ_l = time constant of lead term in compensation networks, sec
ψ_i = input angles to the valves controlling torque about the principal axes, rad
ψ_{0i} = dead zone in valves for the on-off reaction control system about the principal axes, rad
ω_c = crossover frequency of the single-axis attitude control system; it is the frequency at which the Bode diagram crosses the unity-gain line, rad/sec
ω_{di} = desired angular velocities commanded by autopilot, rad/sec
ω_i = vehicle angular velocities measured with respect to inertial space, rad/sec
ω_n = natural frequency of second-order system, rad/sec

Subscripts on i

1 = roll
2 = pitch
3 = yaw

Subscripts on j

1 = star brought to origin
2 = star brought to vertical

Introduction

THE following principles seem to be important to good manual control of a space vehicle:

1) On any display of attitude error, the pilot should see essentially what he sees when he looks out the window: a three part geometric vector.

2) Auxiliary attitude information also should appear graphically as a single "vector" reticle overlaying his window view (or radar display) rather than on separate dials.

Received August 12, 1963; revision received November 20, 1964. Based in part on research at Stanford University under Grant No. NsG-133-61 from NASA, and in part on work performed for Lockheed Missiles and Space Company. Part of the research described in this paper will be included in a thesis to be submitted in partial fulfillment of the requirements for the degree of Doctor of Philosophy.

* Professor of Aeronautics and Astronautics. Member AIAA.

† Senior Scientist, Electronics Sciences Lab.

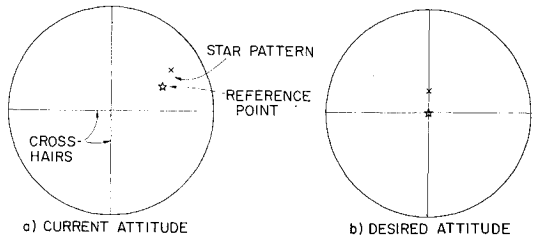

Fig. 1 Attitude control to a star pattern: view through the pilot's window.

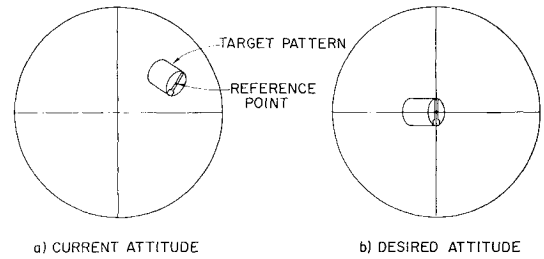

Fig. 2 Attitude control to a target vehicle reference: view through the pilot's window.

3) His control stick should satisfy simultaneously two characteristics: a) a one-to-one correspondence between stick motion and motion of the display and b) a correspondence between stick motion and vehicle rotation that is similar to that in an airplane.

4) The reticle display should respond *instantaneously* (with one-to-one correspondence) to displacement of his control stick.

The rationale behind these four principles is, of course, that displays should not only help the pilot control more quickly and accurately, but should minimize the concentration required of him, and make maximum use of his judgment. Minimization of required concentration improves performance of a particular task, makes available more time and effort for other tasks, and minimizes fatigue. Principles 1 and 2 reduce required concentration because the pilot has only *one place* (rather than multiple dials) to look for *all* of his information, which appears in natural (intuitively grasped) form. Principle 4 reduces required concentration because the pilot does not have to wait to see the results of his control action. Involvement of his judgment is, of course, one principal reason for having him in the control loop at all.‡ A properly designed control arrangement will involve both his decision-making ability and his ability to filter out noise and extraneous signals and to effect more nearly optimum nonlinear control.

The first part of this paper discusses the implementation of principles 1–3. The second part discusses mechanization of the control loop utilizing principle 4 and presents the results of simulator studies in which all four principles are tested. These results are compared with corresponding tests using a number of other techniques, including rate reticle display and quickening. We realize that the matter of manual control of a space vehicle is a highly complex and subjective one. The results of our studies are presented for what interest they may have.

Display and Control Stick Arrangement

Attitude Display

Principle 1 has been recognized for many years. For example, displays being developed for blind landing systems resemble a runway in perspective, so that when the actual runway becomes visible, it appears exactly where the artificial display was. Similarly, in a pursuit aircraft, a radar image of the target may be so displayed optically on the pilot's windshield that if the target is sighted visually it will be exactly behind the optical display. In a space vehicle two typical situations involving manual control are as follows:

i) Attitude control to a star pattern (or planet feature) reference. Figure 1 illustrates control to a two-star pattern; the vehicle is to be rotated about its three axes so that "crosshairs" on the pilot's window point at the brighter star, and the other star appears above it on the vertical. The bright star is the reference point, and the group of stars the reference pattern.

ii) Rendezvous, which includes attitude control (the pilot points his vehicle at the target) and maneuver control (he employs thrust to move laterally about the target). We are concerned here with the attitude control problem. Figure 2a indicates the pilot's view of the target through his window. Prior to starting maneuvers, he points the vehicle so that the face of the target appears as in Fig. 2b. In this case, a line on the face of the target is the reference pattern and the aiming point at the center the reference point.

In either i or ii, and in general, the attitude error is defined in terms of a three-quantity "vector," which the pilot views graphically through his window. Two of the quantities locate the reference point (e.g., the bright star), and the third quantity, an angle, defines orientation of the reference pattern. The three components and their relation to vehicle orientation are defined in Fig. 3. In Fig. 3a, the line of sight to the reference point is shown with respect to the vehicle coordinate frame. (The vehicle axes are numbered in the usual airframe sequence.) The angles α and ϵ (azimuth and elevation) define the direction of the line of sight to the reference point. Quantity ρ indicates a rotation of the reference pattern about its reference point, i.e., the angle between a vertical on the window and a reference line on the pattern. Figure 3b is the pilot's view through a flat window, on which "crosshairs" indicate the directions of the vehicle's *2* and *3* axes. In Fig. 3a point O is the location of the pilot's eyes at distance r from the window; the *1* axis is a line passing through O and the intersection of the crosshairs§ and is assumed to be normal to the window.

The preceding discussion has emphasized the value of principle 1 in relation to a visual outside reference. We wish, at this point, to suggest that principle 1 also is valid when a space vehicle is controlled to a nonvisual reference, i.e., to a radar

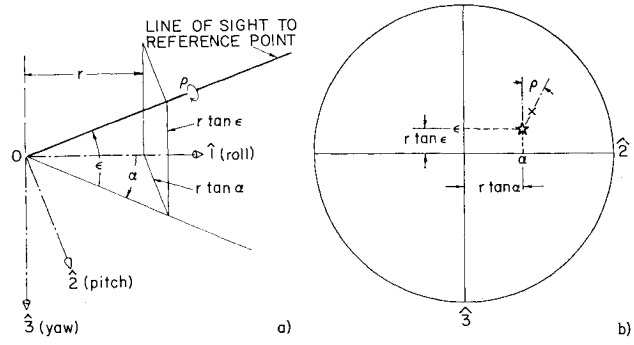

Fig. 3 Error angles and their projection onto a flat window.

‡ Another is that he may be more reliable than the star tracker (or radar), pattern recognition devices, computer, and control components, which would be required in an unmanned system.

§ There is of course a "parallax" problem when the pilot's eye is moved. The reasonable solution is to use virtual image optics to so project the crosshairs on the window that they appear at infinite range.

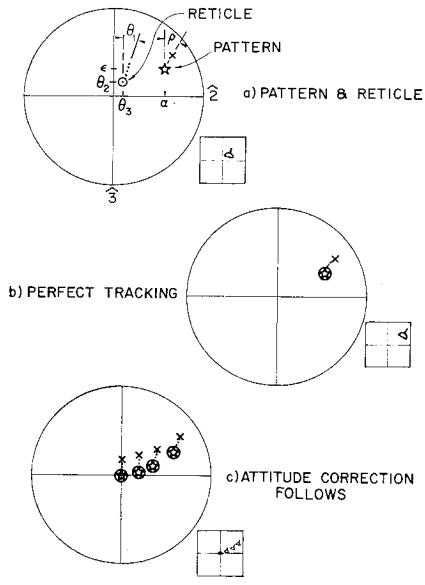

Fig. 4 Tracking a star pattern with a reticle.

signal and/or to a gyro or stable platform (IMU) reference frame. Optical display of the three required quantities on the window (or on a cathode ray tube screen or an "eight ball") in an arrangement that corresponds one-to-one to the natural visual orientation of Fig. 3b should contribute unity and simplicity to the pilot's task.

Vector Rate Reticle

It is often desirable to supply the pilot with auxiliary information. To achieve well-damped control, for example, attitude rate¶ information is usually necessary, particularly in a space vehicle where the basic "plant" produces two pure integrations of input signals. Tests at Stanford have shown that the manual control of such a plant can be greatly improved by making attitude rate information available to the pilot (analogous to rate feedback in a servo), so that he will have to do only one integration mentally instead of two. The question here is how best to display the rate information to him.

Following principle 2, we seek a display that presents all three body rates in a single graphical display and superimposes this display on the window so that the pilot has only one place to look for all of his attitude information. An arrangement that we have used for attitude control to a star pattern is shown in Fig. 4a. The three components of attitude rate about the three axes are all given by the dotted reticle in the same way that the three components of attitude itself are given by location and orientation of the star pattern. Displacement of the dotted reticle to the right (θ_3) is proportional to vehicle yaw rate to the right; displacement upward (θ_2) is proportional to nose-up pitch rate; clockwise rotation (θ_1) is proportional to clockwise roll rate of the vehicle. If the pilot controls the vehicle rate so that the rate reticle is always superposed upon and oriented with the attitude reference as in Fig. 4b, then the vehicle will proceed exactly exponentially to the desired attitude about all three axes simultaneously. (The time constant with which it does so can be adjusted by adjusting the scale factor of the rate reticle.) A typical control sequence is illustrated in Fig. 4c. Note that the pilot has only one quantity to watch: the vector error between the attitude reference pattern and the rate reticle.

¶ This is only an example, because the vector rate reticle to be described does not allow the pilot to see immediately the result of his control action; the control action reticle described later is better.

In practice, pilots using the vector rate reticle tend to modify (improve) the control by moving the controller so as to make the rate reticle overshoot the target initially and then return quickly to the origin just in time to stop the attitude pattern at the origin. Thus, the pilot's "nonlinear" capability is utilized strongly. Moreover, the pilot can filter in a nonlinear, rather optimum way with the aid of the vector display in order to hold attitude in the face of disturbances.

The vector rate reticle represents a substantial advance over the use of separate dials or meters for rate information. However, it does not yet conform to principle 4, because the pilot still must wait through one integration to see the result of his control action. A control action reticle that does respond instantly and exclusively to the pilot's control command is discussed in the next section following a description of the control stick arrangement.

Control Stick and Control Action Reticle

After a number of trials, a control stick arrangement (Fig. 5) has been found that satisfies principle 3 in pitch by providing both a one-to-one correspondence between stick and display and a correspondence to the tradition of pulling the stick back to raise the nose. The stick is mounted horizontally (rather than vertically); pulling it (i.e., raising it) produces nose-up motion. For coordination with the display, the pilot can think of the stick as a pointer that points to the window (or radar screen). Moving the pointer up will move his reticle up, and it will eventually cause the vehicle "crosshairs" to move up.

To preserve this one-to-one correspondence in the other axes we have interchanged the traditional stick functions of yaw and roll. Lateral motion to the right produces vehicle yaw motion to the right; the reticle also moves right and eventually the vehicle crosshairs do too (the little boxes in Figs. 4 and 5 represent location of the stick). Rotation of the stick about its own axis (nominally parallel to the vehicle roll axis) causes the reticle, and eventually the vehicle, to roll in the same way, e.g., clockwise. The pilot is urging the reticle and the vehicle crosshairs to follow the motion of his "pointer."

Although this control stick arrangement minimizes the concentration required to command the appropriate control, the matter of hand-controller design** is independent of the other ideas suggested in this paper. For example, one-to-one correspondence between reticle and vehicle motion can be realized (but less effectively) with a conventional stick grip (with the conventional connection to pitch and roll, and with rotation about the vertical axis, for yaw) if the pilot thinks of it as a pistol that he wants to point at the reference star, with the handle to be aligned with the reference pattern.

To follow principle 4 we must connect the reticle not to vehicle rate or other information, but directly to the control stick, so that the reticle moves instantly, just as if the stick were a flashlight casting the reticle upon the window.†† We call this a control action reticle because it provides control action display (instant feedback) as well as geometric vector display. The "pointing" of the stick to keep the reticle superposed on the target (or other attitude reference) requires very little of the pilot's attention. Stick displacement is arranged to effect proper control action, e.g., to produce gas jet torque on the vehicle through a mechanical or electrical

** Some studies of performance with various control stick arrangements are given, for example, by McRuer and Krendel.[1] It was found that, for the situations experimented with there, the various arrangements are about equally effective at low frequencies.

†† This suggests that the pilot's hand controller and display might be combined by building a reticle mask and optics into the pilot's control stick and projecting a virtual image onto the window.

lead arrangement, which furnishes the required damping to produce good control.

Control Action Display Applied to Satellite Attitude Control

The purpose here is to specify in greater detail, and to demonstrate, the use of the vector reticle display and the hand controller in a three-axis attitude control system. For simplicity we shall consider the case shown in Fig. 1, with the instantaneous location and orientation of the star pattern with respect to the vehicle-fixed coordinate frame defined as in Fig. 3a by angles α, ϵ, and ρ. Equations (1–3) relate the body rates to the relative (observed) angular rates ($\dot{\rho}$, $\dot{\epsilon}$, $\dot{\alpha}$) of the reference pattern:

$$\omega_1 = -\dot{\rho}\cos\alpha\cos\epsilon + \dot{\epsilon}\sin\alpha \quad (1)$$

$$\omega_2 = -\dot{\epsilon}\cos\alpha - \dot{\rho}\sin\alpha\cos\epsilon \quad (2)$$

$$\omega_3 = -\dot{\alpha} + \dot{\rho}\sin\epsilon \quad (3)$$

For small values of α and ϵ, Eqs. (1–3) can be approximated by $\omega_1 \approx -\dot{\rho}$, $\omega_2 \approx -\dot{\epsilon}$, and $\omega_3 \approx -\dot{\alpha}$, respectively. Thus, in a fully automatic control system for "zeroing" α, ϵ, and ρ, a straightforward arrangement would be to "call for" the following desired body rates:

$$\omega_{d1} = K_1\rho \qquad \omega_{d2} = K_2\epsilon \qquad \omega_{d3} = K_3\alpha \quad (4)$$

Equations (4) also provide a reasonable starting point for design of manual control systems.

Rate Command Using Control Action Reticle

By way of introduction to manual control mechanization, we describe first a rate command arrangement that rather closely approximates a fully automatic system.‡‡ The arrangement is depicted, for one axis, in Fig. 6. The pilot uses his control stick to adjust three quantities (δ_1, δ_2, δ_3) to position a reticle (θ_1, θ_2, θ_3) over the reference star pattern, as in Fig. 4b. A control action reticle is connected directly to the stick, so that $\theta_i = K_{ci}\delta_i$ ($i = 1, 2, 3$), and the stick position quantities (δ_1, δ_2, δ_3) serve as inputs to the autopilot rate loops per Eq. (4). This system differs from a fully automatic one only in that the pilot has replaced the star tracker and/or pattern recognition system. If he tracks perfectly, so that the transfer function of the visual tracking loop is a constant, then the characteristic equation of the complete closed-loop system of Fig. 6 (for single-axis operation) is

$$s^2 + (K_{r2}/I_2)s + (K_2K_{r2}/I_2) = 0 \quad (5)$$

and an initial aiming error (for example) can be removed with any desired speed of response and damping. (Practically, the speed of response is limited to 2 or 3 rad/sec by the pilot's dynamic tracking speed as discussed later.)

It may be that the rate command arrangement of Fig. 6 will be deemed unsuitable for manual control of space vehicles because of its reliance on rate gyros or because it is desirable that the pilot have direct mechanical control of the jet valves. In any case, a direct-mechanical-control backup system will be required as an alternative. The next section describes an arrangement that achieves all of the desirable features of the rate command system while using direct pilot control of the jet valves.

‡‡ This arrangement may not be attractive for space vehicle use, as discussed later, but it is quite useful as an introductory illustration. The essence of this rate command arrangement was suggested in 1955 in a patent[2] in which the pilot of a pursuit aircraft tracked an "error dot" image of a target aircraft on a radar screen. His reticle indicated θ_2 and θ_3 (but not θ_1), which were fed into the autopilot as commanded rates.

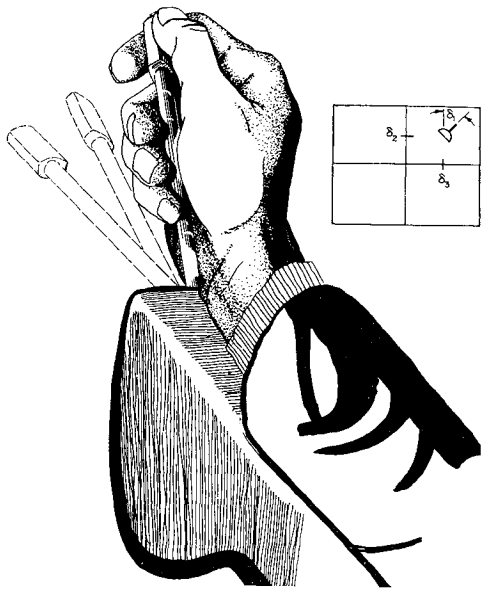

Fig. 5. Control stick.

Control Action Reticle with Direct Valve Control by Pilot: Mechanical Lead Mode

In Project Mercury,[3] two modes of operation were used in which the pilot exercised manual control over gas jets: 1) the three-axis hand controller was connected directly to valves which provided proportional moment control about the three axes, and 2) the hand controller actuated solenoid valves for on-off moment control ("fly-by-wire" mode). However, "Mercury experience to date has indicated that direct manual control over the reaction control thrust nozzles is apt to be quite wasteful of fuel."[4] The two mental integrations between the pilot's display (line of sight angle) and his corrective action (i.e., control torque) apparently resulted in inefficiency due to overshoot and hunting.

We suggest here an arrangement (Fig. 7) in which 1) the control stick is connected mechanically to the jet valves, 2) a control action reticle is used to render the pilot's tracking task simple, and 3) the linkage between the control stick and the valves is constructed to supply a mechanical "lead" so that the system dynamic response is comparable to that of the rate command system previously described. The visual tracking loop is identical to that in Fig. 6, as described in the preceding section. If the pilot tracks perfectly, so that the transfer function of the tracking loop is just a constant, then from Fig. 7a the characteristic equation (for control about a single axis) is

$$\left(\frac{\tau_2}{K_{n2}}\right)s^3 + s^2 + \left(\frac{\tau_2 K_{m2}}{K_{c2}I_2K_{n2}}\right)s + \left(\frac{K_{m2}}{K_{c2}I_2K_{n2}}\right) = 0 \quad (6)$$

By comparison with Eq. (5), if K_{n2} is large and K_{m2} and τ_2 are suitably chosen, the dynamic behavior of this system can be made to approach that of the rate command mode reasonably closely. (A detailed analysis of the dynamic behavior is given later.)

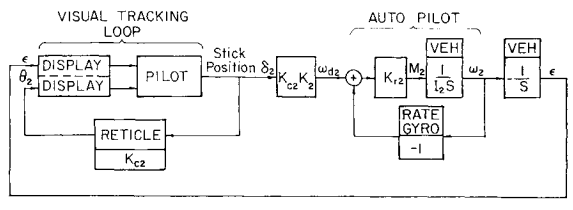

Fig. 6 A rate command manual control arrangement (pitch axis only).

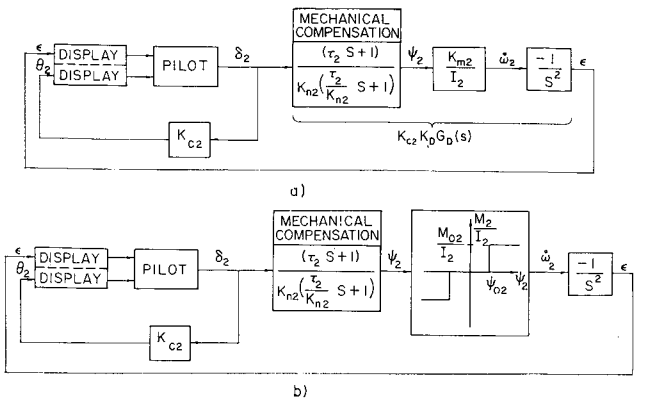

Fig. 7 Block diagram of pitch control system using control action display with a) proportional and b) on-off moment control.

The pilot's control stick is connected to each jet valve through a linkage like that shown in Fig. 8. (The purpose of the dashpot and springs is to process the pilot's response, rather than to provide any kinesthetic feedback to him.) A possible mechanical arrangement is indicated in Fig. 8b. The transfer function, from stick displacement δ_i to valve displacement ψ_i, is readily derived:

$$\frac{\psi_i(s)}{\delta_i(s)} = \frac{[(b/k_1)s + 1]}{[(k_1 + k_2)/k_1]\{[b/(k_1 + k_2)]s + 1\}} = \frac{(\tau_i s + 1)}{K_{ni}[(\tau_i/K_{ni})s + 1]} \quad (7)$$

That is, in Fig. 7 and Eq. (6), $\tau_2 = b/k_1$, $K_{n2} = (k_1 + k_2)/k_1$. For typical desired dynamic behavior the physical constants are reasonable. If the connecting spring and dashpot "freeze up" for any reason, the pilot will still have positive control of the jets. (A cursory study indicates that development of a highly reliable system would be straightforward.) The control moments exerted in response to jet control-valve opening are expressed by Eqs. (8) and (9) for the cases of proportional and on-off moment control, respectively:

$$M_i = K_{mi}\psi_i \qquad i = 1, 2, 3 \quad (8)$$

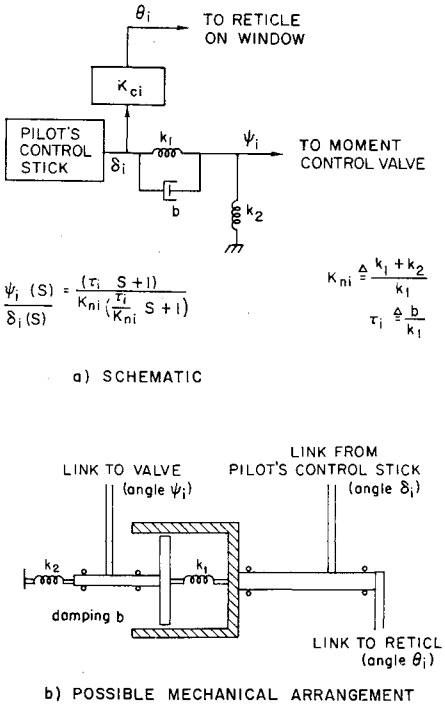

Fig. 8 Mechanical implementation of lead-lag network.

$$M_i = \begin{cases} 0 & \text{for } |\psi_i| < \psi_{0i} \\ M_{0i}\,\text{sign}(\psi_i) & \text{for } |\psi_i| > \psi_{0i} \end{cases} \qquad i = 1, 2, 3 \quad (9)$$

These control moments§§ cause the following angular accelerations:

$$\dot{\omega}_1 = M_1/I_1 + \omega_2\omega_3(I_2 - I_3)/I_1 \quad (10)$$

$$\dot{\omega}_2 = M_2/I_2 + \omega_3\omega_1(I_3 - I_1)/I_2 \quad (11)$$

$$\dot{\omega}_3 = M_3/I_3 + \omega_1\omega_2(I_1 - I_2)/I_3 \quad (12)$$

The control moments applied by the pilot when he positions the reticle reduce the attitude error and cause the stars to rotate (with respect to the vehicle) and move toward the center of the window. Provided that the pilot continues to track the moving star pattern with the reticle, the vehicle will assume a steady-state orientation in which the reference star is located at the center of the window and the other star directly above it.

Single-Axis Analysis of System with Control Action Display

The analysis of the control action display technique is most easily carried out by considering the case in which the motion is restricted to the pitch plane:

$$\alpha(0) = \rho(0) = \omega_1(0) = \omega_3(0) = M_1 = M_3 = 0 \quad (13)$$

Substitution of Eq. (13) into the equations developed in the preceding sections gives the following relationships, which are shown in block diagrams in Fig. 7 and will serve as the basis for discussion throughout the rest of this section:

$$\dot{\epsilon} = -\omega_2 \quad (14)$$

$$\theta_2 = K_{c2}\delta_2 \quad (15)$$

$$\psi_2(s) = \frac{(\tau_2 s + 1)}{K_{n2}[(\tau_2/K_{n2})s + 1]}\,\delta_2(s) \quad (16)$$

$$M_2 = K_{m2}\psi_2 \quad (17)$$

$$M_2 = \begin{cases} 0 & \text{for } |\psi_2| < \psi_{02} \\ M_{02}\,\text{sign}(\psi_2) & \text{for } |\psi_2| > \psi_{02} \end{cases} \quad (18)$$

$$\dot{\omega}_2 = M_2/I_2 \quad (19)$$

It is seen that attitude control systems incorporating control action display consist of an inner loop, which contains the pilot, hand controller, and display, and an "outer loop," which contains the inner loop in addition to the compensation network, moment control system (either proportional as in Fig. 7a or on-off as in Fig. 7b), and vehicle dynamics. The inner loop employs a pursuit display in which the input (ϵ) and output (δ_2) are presented *separately;* it is generally held[5] that superior tracking performance is obtained by using a pursuit display rather than a compensatory display in which only the difference between input and output is displayed.

The pilot's task is to keep $\theta_2 = \epsilon$, so that the transfer function of the entire inner loop containing the pilot, display, and hand controller reduces to a constant gain $(K_{c2})^{-1} = \delta_2/\epsilon$. The consequence of providing feedback around the inner loop by displaying the pilot's control-action is to make the response of the over-all system nearly independent of the elements contained within the inner loop. Factors such as an accurate description of the pilot's transfer function, hand-controller dynamics, and display gain are of only secondary importance. Thus, the design of a manually operated atti-

§§ In these equations, moments due to gravity-gradient, magnetic field, etc. are neglected because they do not contribute significantly to the vehicle motion during the time interval (typically 15 sec) required for an attitude control maneuver.

Table 1 Approximate frequency response of pilot and closed inner-loop

ω, rad/sec	Pilot response, $\frac{\theta_2(s)}{\epsilon(s) - \theta_2(s)}$ Magnitude	Pilot response, Phase, deg	Inner-loop response, $\frac{\theta_2(s)}{\epsilon(s)}$ Magnitude	Inner-loop response, Phase, deg
1	4.5	−81	1.0	−12
2	2.8	−87	1.0	−19
4	1.8	−111	1.0	−33
6	1.3	−137	1.5	−48
8	1.1	−163	3.2	−60

tude control system is reduced to the problem of specifying appropriate compensation for a known plant in order to obtain an acceptable transient response.

In order to make sure that the inner loop functions as a constant gain, it is necessary to choose a compensation network that causes the vehicle to react slowly compared to the pilot, so that his reaction time can be neglected. The transients that he must follow are identically those that would occur in a completely automatic system feeding the attitude error into the compensation network through a gain of $(K_{c2})^{-1}$.

Because a reasonable transfer-function approximation for the pilot's response must include a time delay, it is convenient to make quantitative studies in the frequency domain[6] (the root locus approach, for example, being less convenient in this case). The appropriate compensation can be specified in the frequency domain by requiring that the crossover frequency of the over-all system (i.e., the frequency for which the Bode plot of the outer loop crosses the unity magnitude line) be much lower than the bandwidth of the inner loop. Table 1, derived from the case in Fig. 9, in which the pilot is represented by one of the many transfer functions available in the literature,[1] shows that the closed loop containing the display, pilot, and hand controller contributes negligibly to the dynamics of the over-all system for frequencies lower than 2.0 rad/sec.

Reference to Fig. 7a (the system employing proportional moment control) shows that the open loop transfer function of the outer loop is given by

$$KG(s) = \underbrace{\frac{1}{K_{c2}} \frac{\theta_2(s)}{\epsilon(s)}}_{\text{Transfer function of inner loop}} \cdot \underbrace{\frac{\epsilon(s)}{\delta_2(s)}}_{\text{Transfer function of compensation and vehicle dynamics}} \tag{20}$$

Equation (20) is rewritten in the following form, which separates the parameters under control of the designer from the response determined by the pilot:

$$\left.\begin{aligned} KG(s) &= \underbrace{\left[\frac{K_{m2}}{K_{c2}K_{n2}I_2} \cdot \frac{(\tau_2 s + 1)}{s^2[(\tau_2/K_{n2})s + 1]}\right]}_{\text{Specified by designer}} \times \underbrace{\frac{\theta_2(s)}{\epsilon(s)}}_{\text{Determined by pilot}} \\ KG(s) &= K_d G_d(s) \frac{\theta_2(s)}{\epsilon(s)} \end{aligned}\right\} \tag{21}$$

where

$$K_d = K_{m2}/K_{c2}K_{n2}I_2 \tag{22}$$

$$G_d(s) = (\tau_2 s + 1)/s^2[(\tau_2/K_{n2})s + 1] \tag{23}$$

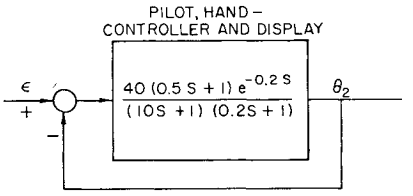

Fig. 9 Representation of pilot as a linear transfer function.

Provided that a crossover frequency much lower than 2 rad/sec is chosen, the appropriate time constant and gain are

$$\tau_2 = K_{n2}^{1/2}/\omega_c \tag{24}$$

and

$$K_d = \omega_c^2 K_{n2}^{-1/2} \tag{25}$$

Figure 10 is a Bode diagram for a typical ($K_{n2} = 10$) single-axis system, in which τ_2 and K_d were chosen to give $\omega_c = 0.5$ rad/sec. It shows that the inner loop contributes negligibly to the dynamics near the crossover frequency ω_c, and therefore the closed loop response is determined primarily by the compensation network and vehicle dynamics.

The use of control action display for an on-off moment control is illustrated by Fig. 7b. The stick (in addition to moving the reticle on the window) is coupled through a spring and dashpot (Fig. 8) to on-off jet valves. The closed-loop response is determined primarily by the values of M_{02}/I_2 and τ_2 because the inner loop acts as a constant gain. The proper choice of M_{02}/I_2 and τ_2 can be explained by referring to Fig. 11. The optimum (i.e., minimum response time) switching line is

$$\dot{\epsilon} + [2(M_{02}/I_2)\,|\epsilon|]^{1/2}\,\text{sign}(\epsilon) = 0 \tag{26}$$

Although this equation could be implemented using a nonlinear spring and/or dashpot, quite adequate performance can be obtained using the linear approximation $\tau_2\dot{\epsilon} + \epsilon = 0$, wherein τ_2 is chosen such that the approximate switching line intercepts the optimum switching line on the trajectory starting from a nominal offset angle. The rate gain and angular acceleration can be expressed in terms of the minimum transient time $\tau_2 = T/4$ and the nominal offset angle $M_{02}I_2 = 4\epsilon(0)/T^2$. Trajectories starting at greater (less) than $\epsilon(0)$ intersect the approximate switching line too late (early) and require more than one thrust reversal and slightly greater than the minimum time to reach null; the presence of a lag term in the compensation network and the thrust dead zone also degrade the performance slightly. At the end of the acquisition phase (during which a large initial offset is brought within the thrust control valve dead zone) a small residual angular velocity may be present. During the subsequent station-

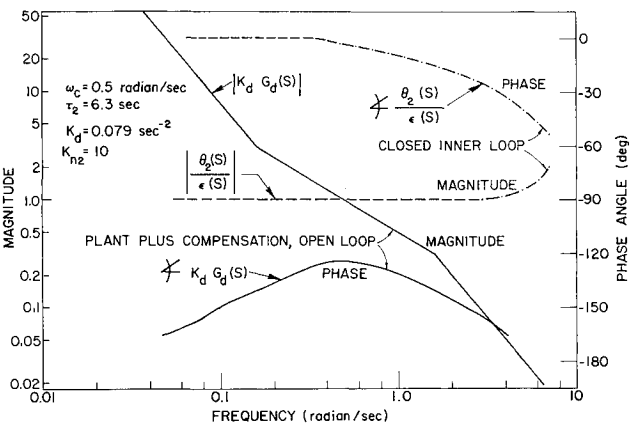

Fig. 10 Bode diagram of typical system.

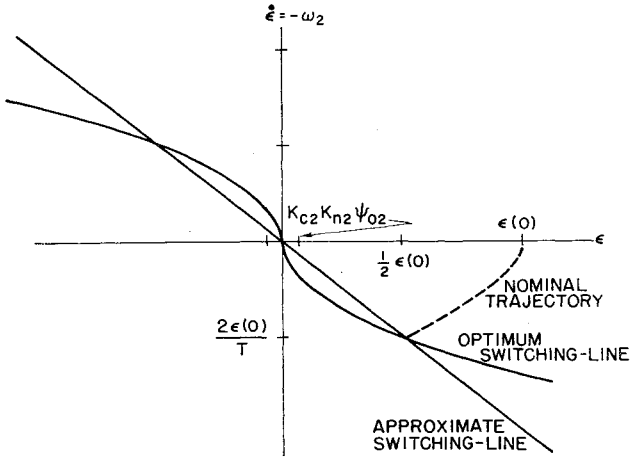

Fig. 11 Phase-plane analysis of on-off control system.

keeping phase, the pilot can reverse this velocity by applying very short (~0.1 sec) bursts of thrust whenever the vehicle attitude drifts beyond some prescribed tolerance. In this way he causes the vehicle to follow a stable limit cycle of the type described by Gaylord and Keller.[7]

Comparison with Other Techniques for Manual Control

It was shown in the previous section that the dynamic behavior of the rate command scheme using the control action reticle and of the mechanical lead scheme are essentially the same; therefore, the analysis and conclusions of that section apply to both systems.

Quickening[8, 9] is a technique that has been applied with considerable success in a wide variety of manual control applications. Figure 12 illustrates the use of quickening in single-axis attitude control systems employing proportional and on-off jet controls. The reticle is driven by a weighted sum of angular acceleration and angular rate about the principal axes:

$$\theta_2 = D_{12}\omega_2 + D_{22}\dot{\omega}_2 \tag{27}$$

The pilot's task is to keep the reticle superimposed over the stars, so that $\theta_2 = \epsilon$, in which case the transfer function between attitude error and vehicle angular acceleration is

$$\dot{\omega}_2(s)/\epsilon(s) = s/D_{12}[(D_{22}/D_{12})s + 1] \tag{28}$$

and the open loop transfer function of the single-axis system is

$$KG(s) = \{D_{12}[(D_{22}/D_{12})s + 1]s\}^{-1} \tag{29}$$

If the display gains are chosen to be $D_{12} = 2\zeta\omega_n^{-1} = 2$ sec

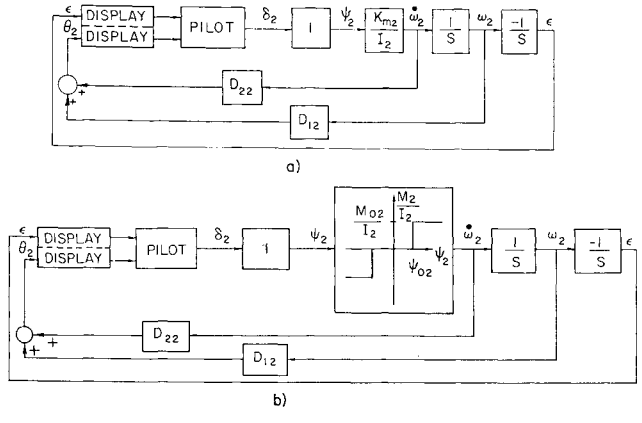

Fig. 12 Block diagram of pitch control system using quickening or rate-reticle display with a) proportional and b) on-off moment control.

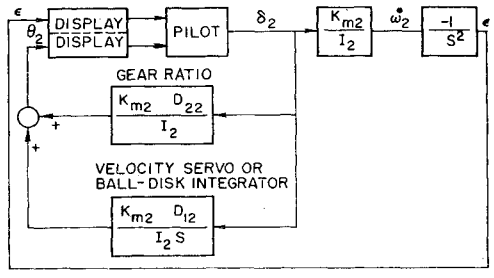

Fig. 13 Alternative implementation of quickened system.

and $D_{22} = \omega_n^{-2} = 2.8$ sec^2, the closed loop system will respond as a second-order system having a natural frequency ω_n and a damping-ratio ζ; the numerical values apply to a typical case in which the natural frequency is 0.6 rad/sec and the damping ratio is 0.6.

Setting D_{12} equal to zero results in an unstable system. From the open loop transfer function given by Eq. (29), it can be seen that setting D_{22} equal to zero results in a system that exhibits a first-order response with a time constant equal to D_{12}; this is the case of the rate reticle display suggested by Cannon.[10]

Comparison of Figs. 7 and 12 indicates that quickening differs from control action display in two important respects:

1) No compensation is used between the pilot and the jet control valves; the compensation (specifically, the filtered derivative) required to stabilize the system is obtained in the inner loop by operation of the display [Eq. (28)].

2) Comparison of Eq. (15) with

$$\theta_2(s) = D_{12}\omega_2(s) + D_{22}\dot{\omega}_2(s) = \frac{K_{m2}}{I_2}\left(D_{22} + \frac{D_{12}}{s}\right)\delta_2(s)\text{¶¶} \tag{30}$$

indicates that the open loop dynamics of the inner loop are more complex in the case of quickening and rate reticle ($D_{22} = 0$) than for control action display. The reticle position is determined not only by the pilot's instantaneous response but also by a component that is proportional to the

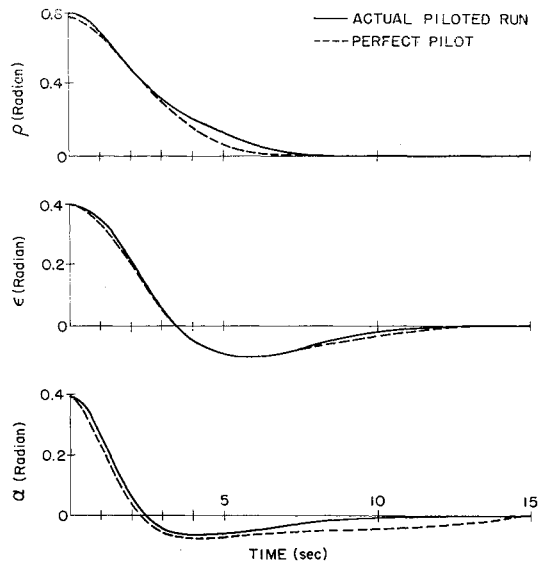

Fig. 14 Transient response of system using control action display with proportional moment control.

¶¶ Equation (30) suggests the possibility of mechanizing the quickened system according to Fig. 13, thereby avoiding the necessity of providing velocity and acceleration sensors on each of the three axes.

integral of his past responses (i.e., $D_{12} \neq 0$). The types of tracking employed within the inner loop are known as "direct," "aided," and "velocity" tracking in the case of control action display, quickening, and rate reticle, respectively. Lincoln and Smith[11] have shown that direct pursuit tracking is consistently more accurate than aided tracking and that velocity tracking is very poor in comparison with both of the others. In the case of on-off moment control (Fig. 12b), the on-off characteristic is also contained within the inner loop. The introduction of this gross nonlinearity in the display loop makes it nearly impossible for the pilot to track the designated stars with the reticle.

Still another technique used in the design of manually controlled systems is Kelly's[12] "predictor instrument." This approach displays the predicted time history of the system errors computed by an analog computer model of the plant operating many times faster than real time; the prediction is made under the assumption that the controller is returned to zero at that instant of time. This approach differs from control action display in two respects: 1) the display does not indicate what corrective action the pilot should take but instead displays the transient that will result if no corrections are applied (coding is required in order to display multidimensional transients in two dimensions); and 2) the attitude errors and body rates must be available as electrical inputs to the fast-time analog computer (a star tracker would be required to convert a visual reference into electrical signals).

Simulation of Three-Axis Attitude Control

An analog-computer study was performed to determine the effectiveness of control action reticle, quickening and rate reticle in a three-axis attitude control system.* In this fixed-base simulation, the pilot's view of the star field and reticle (Fig. 4a) was presented on an oscilloscope. The coordinates of stars no. 1 and no. 2 were generated from the equations

$$\dot{\alpha}_j = -\omega_3 - \epsilon_j\omega_1 \qquad j = 1, 2 \tag{31}$$

$$\dot{\epsilon}_j = \alpha_j\omega_1 - \omega_2 \qquad j = 1, 2 \tag{32}$$

which can be derived using Eqs. (1–3) and small angle approximations for α and ϵ. For this case $\dot{\rho}$ reduces to $-\omega_1$; this relationship was not used explicitly in the simulation, however. The cross-coupling due to differences in principal moments of inertia [see Eqs. (10–12)] was neglected in the derivation of body rates about the three axes. The reticle was positioned according to Eqs. (33) and (34) for control action reticle and quickening, respectively:

$$\theta_i = K_{ci}\delta_i \qquad i = 1, 2, 3 \tag{33}$$

$$\theta_i = D_{1i}\omega_i + D_{2i}\dot{\omega}_i \qquad i = 1, 2, 3 \tag{34}$$

(Recall that rate reticle is a special case of quickening in which $D_{2i} = 0$.) Sampling of the variables in the oscilloscope display at 20 samples/sec by an electromechanical commutator gave a flicker-free presentation. The pilot controlled the spacecraft using a spring-restrained, three-axis controller similar to the one illustrated in Fig. 5. Figures 14–22 show typical results of a maneuver defined by the initial conditions

$$\alpha_1(0) = \epsilon_1(0) = 0.4 \text{ rad} \qquad \alpha_2(0) = \epsilon_2(0) = 0.5 \text{ rad}$$
$$\omega_1(0) = \omega_2(0) = \omega_3(0) = 0 \tag{35}$$

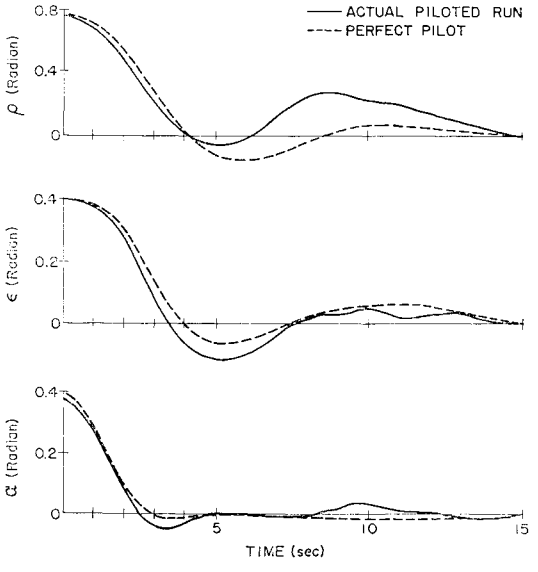

Fig. 15 Transient response of system using control action display with on-off moment control.

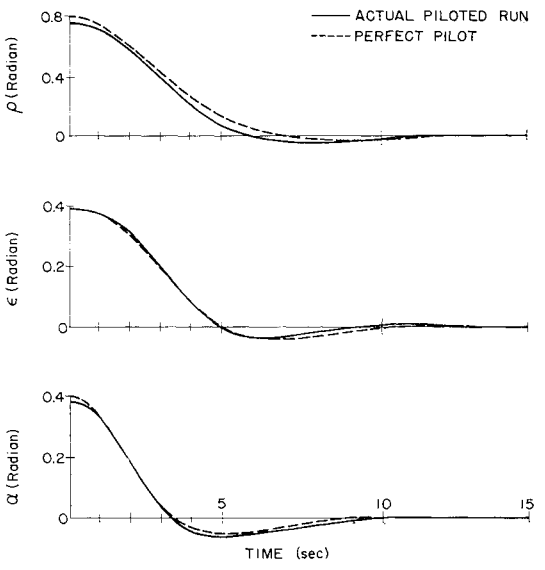

Fig. 16 Transient response of system using quickening with proportional moment control.

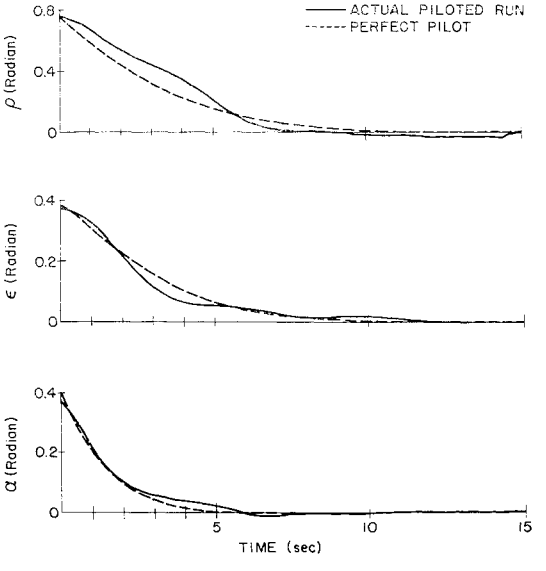

Fig. 17 Transient response of system using rate reticle with proportional moment control.

* Earlier experimental work by Florance[13] and O'Grady[14] at Stanford University has demonstrated the superiority of a vector reticle display over a set of three single-axis displays (dials). Additional experiments with dials were therefore not included in the present studies.

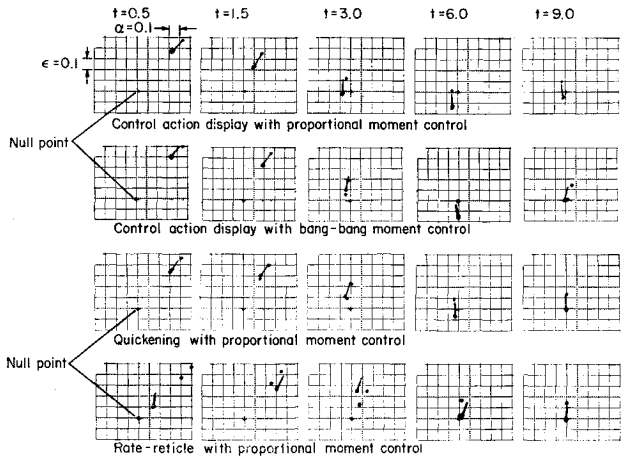

Fig. 18 Pilot's display at selected times during attitude control maneuver.

with the parameters listed in Table 2. It is emphasized that, since control action display can be mechanized either as a rate command system or as a lead compensation system (which can use mechanical compensation entirely, Fig. 8), the two being mathematically the same, the simulation results described here represent both mechanizations. The system constants given in Table 2 are for the compensation arrangement, but equivalent rate command constants can be deduced from the earlier discussion.

Figures 14–17 show the line-of-sight angles to the reference star as functions of time for the maneuver defined by Eq. (35). These particular runs were selected from several trial runs for each system because they closely approximate the transient performance that would have resulted if the pilot had kept the reticle perfectly aligned over the star pattern throughout the entire maneuver. The transient responses for the so-called "perfect pilot," given by the dashed curves in Figs. 14–17, were obtained by connecting the appropriate error signals directly to the control jet inputs (in place of the control stick outputs δ_i) so that the reticle was always superimposed over the star pattern. Since corrections were applied in roll, pitch, and yaw simultaneously, the transient response in each axis is considerably different from that derived on the basis of the single-axis analysis given in two preceding sections. For example (in this particular maneuver),

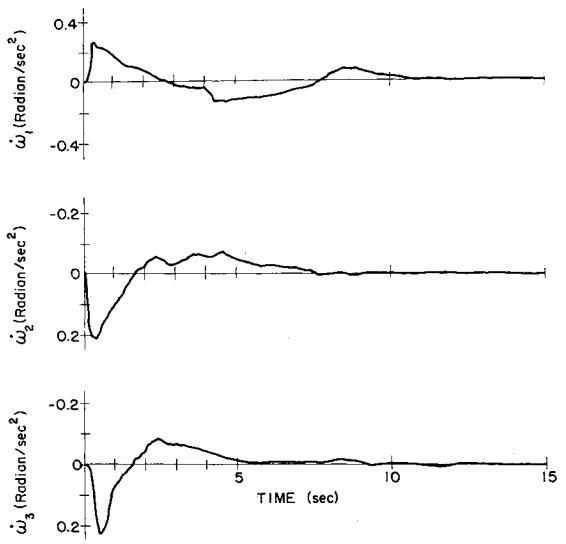

Fig. 19 Angular accelerations for system using control action display with proportional moment control.

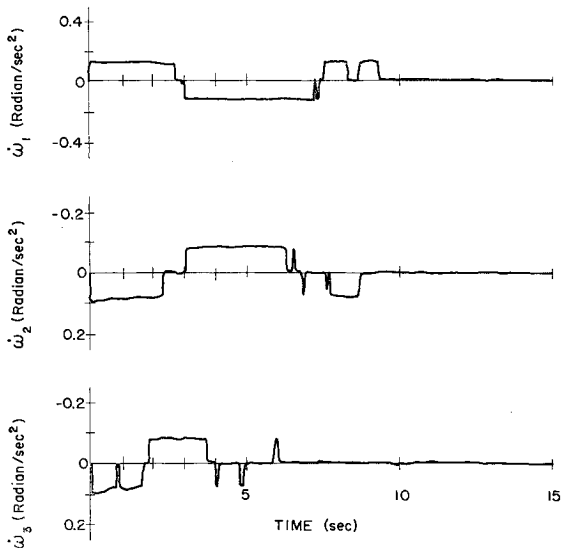

Fig. 20 Angular accelerations for system using control action display with on-off moment control.

roll motion is strongly coupled into yaw with the result that errors in α are reduced much more rapidly than errors in ϵ.

For the perfect pilot, similar transient behaviors are obtained from systems using control action display and quickening with proportional moment control (Figs. 14 and 16); both are typical second-order responses with moderate overshoot and approximately equal duration. The overshoot is a little greater in the case of control action display using on-off moment control; this occurs (Fig. 15) because the approximate switching line (see Fig. 11) was derived for initial conditions somewhat different from those that were actually used. The system using rate reticle with proportional moment control exhibits typical first-order response (Fig. 17).

Figure 18 shows the pilot's display† at designated instants of time during the specific runs shown in Figs. 14–17. Tracking was moderately accurate for all of these runs. However, on the basis of the limited number of experiments performed

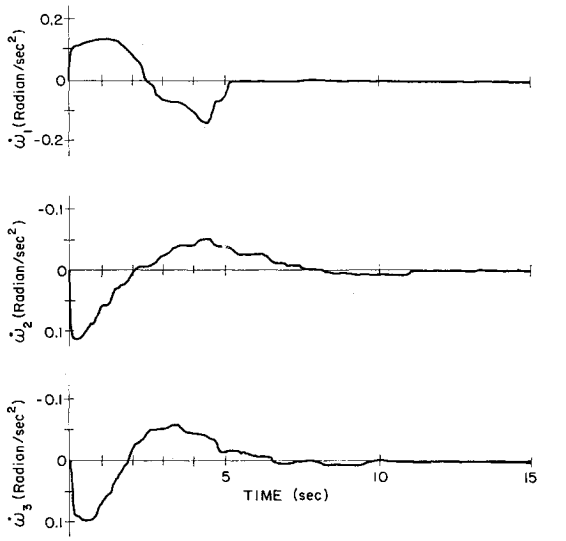

Fig. 21 Angular accelerations for system using quickening with proportional moment control.

† The grid markings in the oscilloscope presentation would not be a part of the pilot's display in the actual system. They are presented in these photographs to permit a quantitative evaluation of the data.

to date, it appears that, for the manual control of spacecraft using proportional moment control, control action display is somewhat superior to quickening and substantially superior to rate reticle display. This ranking, which relates to the ease with which the pilots tested can perform various attitude control maneuvers, is in agreement with the results of Lincoln and Smith,[11] who found that direct pursuit tracking was somewhat better than aided tracking, which was in turn better than velocity tracking. Moreover, tracking with the control action display is more consistent than with quickening: the response of Fig. 14 is typical of most of the runs with control action display, whereas runs with quickening were not often as good as Fig. 16. The advantage of control action display over the other two techniques is outstanding in the case of systems employing on-off moment control.

Figures 19–22 show angular accelerations as functions of time about each of the three principal axes for selected runs (although not the same runs as in Figs. 14–18) using each of the four systems. Relative fuel consumptions estimated from the areas (absolute value) under these curves, appear to be approximately the same for all cases except rate reticle, which required somewhat more fuel. Previous work at Stanford[13,14] demonstrated, however, that systems using the vector rate reticle required less fuel than systems that display auxiliary information on separate dials. In practice, for systems using control action display or quickening, the time allowed for the maneuver is more important than the detailed response characteristics, because the fuel required varies inversely with this maneuver time.

Summary

Two concepts have been studied for manual attitude control: 1) the vector reticle for displaying auxiliary information about all three axes in a single, graphical entity superimposed on the pilot's field of view; and 2) control action display, which gives the pilot instantaneous feedback on the correctness of his control action, thus minimizing the concentration required for his tracking task. The two concepts are combined in the *control action reticle* with which good dynamic behavior can be realized in spacecraft employing either proportional or on-off moment control.

A single-axis analysis showed that displaying the pilot's instantaneous response has the effect of providing a tight feed-back loop around the pilot, hand controller, and display; this feedback causes that section of the system to act as a constant gain despite variations in pilot response. The response of the system is determined primarily by the dynamics of the vehicle and compensation network. The designer selects a compensation network to obtain a satisfactory system response, subject to the constraint that the system must react slowly enough to allow the pilot to track the stars with the reticle. Compensation networks suitable for systems employing both proportional and on-off thrust control were derived.

An all-mechanical compensation device is suggested which gives the pilot direct control of the jet valves, so that the entire control system can be implemented with only mechanical components. A control stick arrangement is suggested which further unifies and simplifies the pilot's task with minimum change from the traditional arrangement.

Simulation studies indicated that the best runs for systems using control action display, quickening, and rate reticle exhibit comparable transient responses and require approximately the same amount of fuel for a given maneuver. However, more consistent results are obtained with less effort when using control action display. Furthermore, control action display makes it possible to control spacecraft employing *on-off moment control* (probably the case of greatest interest) almost as well as spacecraft employing proportional moment control.

Table 2 Parameters used in simulation of 3-axis attitude control systems

Parameter	Axis		
	Roll	Pitch	Yaw
Figs. 14, 18, and 19:	control action display with proportional moment control		
K_c	3.0	1.25	1.25
K_m/I, sec^{-2}	1.5	1.0	1.0
τ, sec	7.9	6.3	6.3
K_n	10	10	10
Figs. 15, 18, and 20:	control action display with on-off moment control		
K_c	3.0	1.25	1.25
M_0/I, rad/sec^2	0.12	0.08	0.08
ψ_0, rad	0.004	0.004	0.004
τ, sec	1.25	1.25	1.25
K_n	10	10	10
Figs. 16, 18, and 21:	quickening with proportional moment control		
D_1, sec	2.5	2.0	2.0
D_2, sec^2	3.5	2.8	2.8
K_m/I, sec^{-2}	0.4	0.4	0.4
Figs. 17, 18, and 22:	rate-reticle display with proportional moment control		
D_1, sec	3.5	2.5	2.5
D_2, sec^2	0	0	0
K_m/I, sec^{-2}	0.2	0.2	0.2

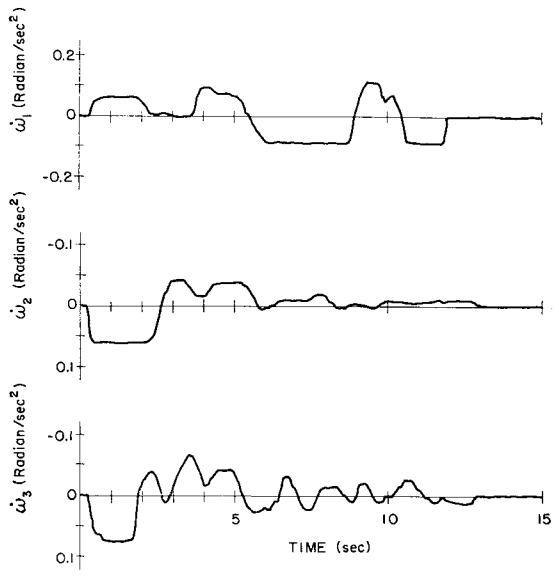

Fig. 22 Angular accelerations for system using rate reticle with proportional moment control.

References

[1] McRuer, D. T. and Krendel, W. N., "Dynamic response of human operators," Wright Air Development Center TR 56-524 (1957).

[2] Campbell, M. E., "Tracking display for aircraft," U. S. Patent No. 2,943,824 (July 5, 1960).

[3] Iwombly, J. W., "The Mercury capsule attitude control system," *Proceedings of the National Meeting on Manned Space Flight* (Institute of The Aerospace Sciences, New York, 1962), pp. 228–231.

[4] Bailey, F. J., Jr., "Review of lessons learned in the Mercury program relative to spacecraft design and operation," AIAA Paper 63073-63 (March 1963).

[5] Senders, J. W. and Cuzen, M., "Tracking performance on combined compensatory and pursuit tasks," Wright Air Development Center TR 52-39 (1952).

[6] Grabbe, E. M., Ramo, S., and Wooldridge, D. E., *Handbook of Automation, Computation, and Control* (John Wiley and Sons, Inc., New York, 1958), Vol. 1, Chap. 22.

[7] Gaylord, R. S. and Keller, W. N., "Attitude control system using logically controlled pulses," *ARS Progress in Astronautics and Rocketry: Guidance and Control*, edited by R. E. Roberson and J. S. Farrior (Academic Press, New York, 1962), Vol. 8, pp. 629–648.

[8] Birmingham, H. P. and Taylor, F. V., "A human engineering approach to man-operated continuous control systems," U. S. Naval Research Lab. Rept. 4333, Washington, D. C. (1954).

[9] Birmingham, H. P. and Taylor, F. V., "Why quickening works," Paper 58-AV-9, American Society of Mechanical Engineers (March 17, 1958).

[10] Cannon, R. H., "A new vector rate reticle display for manual control of space vehicle attitude and rendezvous maneuvers," Lockheed Missiles and Space Co. Rept. A385590 (August 1963).

[11] Lincoln, R. S. and Smith K. V., "Systematic analysis of factors determining accuracy in visual tracking," Science **116**, 183–187 (1952).

[12] Kelly, C. R., "Developing and testing the effectiveness of the predictor instrument," et seq., Dunlap and Associates, Inc., Stamford, Conn., TR 252-60-1 et seq. (1960).

[13] Florance, J. E., Jr., "Vewar—An attitude display system for a pilot-controlled space vehicle," Stanford Univ., unpublished report (1961).

[14] O'Grady, J. W., "Fabrication of a three axis control system simulator," Stanford Univ., unpublished report (1963).

MARCH-APRIL 1965 J. SPACECRAFT VOL. 2, NO. 2

Vibration Isolation Effectiveness of Inertia Pads Resting on Soil

GEORGE W. KAMPERMAN*
Bolt Beranek and Newman, Inc., Downers Grove, Ill.

Large concrete inertia pads resting on soil are commonly believed to provide a high degree of isolation from ground vibration. Our vibration measurements on existing installations show that inertia pads provide little or no vibration isolation in the frequency range below about 20 cps. Vibration spectra measured on and off inertia pads are presented. A simple passive vibration isolation system using springs is considered.

Introduction

RAPID progress is being made in the performance of inertial instruments; there is approximately a ten-fold improvement in the null stability and threshold performance every five years. At present, gyro uncertainty ranges between 10^{-3} and 10^{-4} deg/hr, and accelerometer uncertainty, or threshold, ranges between 10^{-5} and 10^{-6} g. To evaluate effectively the performance of gyros and accelerometers in inertial guidance systems, it is essential that the testing platform have a stability comparable to or better than the instruments being tested.

The purpose of the present study was to establish design criteria for inertia pads to be mounted on earth at the new Guidance, Control, and Aeroballistic Facility at the Redstone Arsenal at Huntsville, Ala. The study comprised four phases: 1) review of data from various locations in the United States to determine the level of the microseisms that may be expected at the Huntsville site, 2) measurements at the Huntsville site to determine amplitude-frequency characteristics of the earthborne cultural noise (man-made vibration), 3) investigation of the vibration-isolation properties of inertia pads resting on earth, and 4) development of a design philosophy for the inertia pads to be constructed at Huntsville.

Ground Vibration

Under Project VELA-UNIFORM, as part of the U. S. Nuclear Test Detection System, several seismological observatories have been established in remote, seismically quiet areas. Ground vibrations in the frequency range from 0.001 to 10 cps are detected and recorded at these observatories. The level of the microseisms at these observatories is generally less than 10^{-7} g over this frequency range.[1] From discussions with several seismologists, we have concluded that the natural ground vibrations (other than earthquakes) at the Huntsville site will not exceed 10^{-6} g peak-to-peak acceleration.[2, 3] Therefore, the ground vibration sources of principal interest are vehicle traffic and other local man-made disturbances,[4] such as test firings of large rocket engines in other areas of the Arsenal.

Vibration from Trains

In December 1962, personnel from the U. S. Army Engineer Waterways Experiment Station under the Corps of Engineers at Vicksburg, Miss., made measurements at the Redstone Arsenal[5] to determine the ground vibration caused by a moving train 2000 ft from the desired test site. Because of inherent limitations in the sensitivity of the available instrumentation, they were unable to detect vibration at the site, but useful measurements were obtained at distances of 50, 250, and 500 ft from the railroad track. Acceleration measurements were made simultaneously in the three mutually perpendicular axes. The maximum peak-to-peak acceleration and predominant characteristic frequency were recorded as the train passed the measuring station at speeds up to 25 mph. Measurements were made for the train engine alone and for the engine plus several loaded cars. Fifty feet from the track, the maximum peak-to-peak acceleration ranged from 10^{-2} to 10^{-1} g. At 250 ft, the range was 10^{-3} to 10^{-2} g; at 500 ft, 2×10^{-4} to 1.7×10^{-3} g. The amplitude was approximately the same in the vertical and horizontal directions. The predominant frequencies ranged between 16 and 33 cps. From these measurements, the Vicksburg group estimated the peak-to-peak vibration at the site 2000 ft from the track to be approximately 10^{-6} g with the train operating as described previously.

Received January 15, 1964; revision received December 7, 1964.

* Supervisory Consultant.